Dynamical feedbacks and the persistence of the NAO

Elizabeth A. Barnes * and Dennis L. Hartmann

Department of Atmospheric Sciences, University of Washington, Seattle, Washington

* *Corresponding author address:* Elizabeth A. Barnes, Department of Atmospheric Sciences, University of Washington, Box 351640, Seattle, WA 98195.

E-mail: eabarnes@atmos.washington.edu

ABSTRACT

The persistence of the North Atlantic Oscillation (NAO) is studied using observations of the three-dimensional vorticity budget in the Atlantic sector. Analysis of the relative vorticity tendency equation shows that convergence of eddy vorticity flux in the upper troposphere counteracts the effect of anomalous large-scale divergence at the upper level. At low levels, the convergence associated with this large-scale vertical circulation cell maintains the relative vorticity anomaly against frictional drag. The eddy vorticity flux convergence thus acts to sustain the vorticity anomaly associated with the NAO against drag and increases the persistence of the NAO vorticity anomaly. The adiabatic cooling associated with the rising motion in the vorticity maximum also sustains the thermal structure of the NAO anomaly. This constitutes a positive eddy feedback that helps maintain the NAO. The positive eddy feedback occurs only in the mid-latitude region and is strongest when the Atlantic jet is displaced toward the equator, with a high pressure anomaly to the north and a low pressure anomaly to the south. The stronger feedback demonstrated in the case where the jet is displaced toward the equator is consistent with the greater persistence observed for this phase of the NAO. The positive feedback appears to be associated with anomalous northward eddy propagation away from the jet.

1. Introduction

In 1924, Gilbert T. Walker coined the name "North Atlantic Oscillation" (NAO) for the well-known swaying of pressure anomalies between the Azores and Iceland (Walker 1924). Today, this teleconnection pattern is known to be a poleward (equatorward) shift of the Atlantic jet when the NAO is in its high- (low-) phase. This oscillation affects the weather over western Europe and Greenland. While Feldstein (2000) found the e-folding time of the NAO to be approximately 10 days, Rennert and Wallace (2009) argue that it is not the e-folding time, but rather the persistence beyond 30 days that distinguishes this pattern. The results presented here provide a possible explanation for this extended persistence.

The distinction between the NAO and the hemispheric variability of the Northern Hemisphere extratropical jet, coined the Northern Annular Mode (NAM), has been a topic of debate (Thompson and Wallace

1998, 2000; Ambaum et al. 2001). In the zonal-mean, the annular mode in each hemisphere manifests itself as a latitudinal shifting of the eddy-driven jet (Lorenz and Hartmann 2001, 2003) (LH01 and LH03 hereafter). The zonal-mean variation of the jet associated with the Northern Annular Mode during winter was shown by LH03 to have an increased persistence due to a positive eddy-zonal flow feedback. In their work, LH03 were able to pinpoint the synoptic eddies (high-pass 15-day filter) as the main contributors to this positive feedback, as suggested also by Feldstein and Lee (1998). They also demonstrated that the second leading mode of variability (2nd monthly-mean EOF of zonal flow), associated with a strengthening and sharpening of the jet, had a weak feedback and thus lacked the persistence of the leading mode.

Building from the work of LH03, Eichelberger and Hartmann (2007) studied the leading mode of variability for zonally averaged flow in the Atlantic and Pacific sectors during Northern Hemisphere winter. They found that the first EOF of the Atlantic corresponded well with the NAM while the first EOF of the Pacific was a combination of a latitudinal shifting and a pulsing of the jet. Eichelberger and Hartmann (2007) proposed that the amplitude of the annular mode over the Pacific sector is reduced due to the weak eddy-zonal flow feedbacks associated with a stronger Hadley-driven subtropical jet. These feedbacks were weakened in the strong subtropical jet due to the stronger waveguide inhibiting the propagation of waves away from the source region (inhibiting momentum flux into the jet).

Holopainen and Oort (1981) demonstrated that transient eddy forcing in the mid-latitudes reinforced the time-mean vorticity patterns against surface drag, leading to the maintenance of dominant disturbances such as the North Pacific low, North Atlantic low and the Siberian high. In more recent work, Robinson (1996, 2000) demonstrated the importance of surface drag to the eddy-feedback interaction responsible for the extended persistence of the zonal-index. With a poleward shift of the jet, the eddy fluxes produce a poleward transport of heat which typically reduces the baroclinicity in the region of the shifted jet (and thus restricts the production of more eddies). However, in the presence of drag, the poleward transport of heat and, thus, destruction of the temperature gradient, is balanced by the adiabatic cooling from a thermally induced Ferrel cell which moves momentum supplied by eddy fluxes at upper levels to the surface (Robinson 2006; Hartmann 2007).

The positive-feedback mechanisms described thus far have all been in a zonal-mean framework. Feldstein

(2003) used the 300 mb stream-function to investigate the life cycle of the North Atlantic Oscillation (NAO). He performed composite analysis on each term in the stream-function tendency equation to demonstrate that even after the anomaly pattern attains its maximum amplitude, the high-frequency (10-day filtered) eddy forcing continues to project positively onto the pattern. We demonstrate that the net eddy flow of vorticity constitutes a positive feedback that together with the implied vertical motion field makes the NAO anomalies self-sustaining.

2. Data

The data consists of 43 years (1959-2001) of 2.5×2.5 latitude-longitude gridded daily (1200 UTC) sea-level pressure (SLP), zonal velocity (u), meridional velocity (v) and the vertical component of relative vorticity ($\zeta = \nabla \times \mathbf{u}$ where $\mathbf{u} = (u, v)$) on 13 vertical levels (1000, 925, 850, 775, 700, 600, 500, 400, 300, 250, 200, 150 and 100 mb) from the European Centre for Medium-Range Weather Forecasts Re-Analysis (ERA-40) (Uppala et al. 2005). Only Northern Hemisphere winter-time (Dec.-Mar.) fields are analyzed in this paper, and the time series analysis is applied to each 121 winter season of DJFM (thus ignoring March 31 during leap-years).

To analyze the variability of the atmosphere, the mean seasonal cycle is removed from the daily climatology of the data field. The mean seasonal cycle is a smooth curve computed as the annual mean plus the first four Fourier harmonics of the daily climatology. Thus, the magnitude of a variable x at a single location can be decomposed into a climatological value $\overline{x}$ plus an anomalous value $\hat{x}$. Part of this analysis requires splitting the anomalous fields into high- and low-frequency components, representing variability on times-scales less than and greater than 7 days respectively. This frequency division used a 7-day cutoff Lanczos filter with 41 weights (Hamming 1989) applied to the full 43 years of anomalies for each field.

3. Low-frequency variability in the Atlantic sector

The NAO pattern explains the largest amount of the variance of DJFM low-frequency sea-level pressure variability over the Atlantic. Empirical Orthogonal Function analysis of the monthly-mean sea-level pressure anomalies in the Atlantic sector (25^o-87.5^oN, 90^oW-30^oE) results in a leading pattern for which we define the positive phase to be a low-pressure center over Greenland and a high-pressure center in the mid-latitudes of the Atlantic Ocean as shown in Fig. 1. The structure is displayed in units of mb and not in normalized form, and explains 38% of the monthly variability of winter sea-level pressure in the Atlantic sector. Before performing EOF analysis, the data was properly weighted to account for the decrease in area toward the pole. The structure obtained is not sensitive to the exact Atlantic region used and is unique according to the criteria outlined by North et al. (1982).

The following results use an NAO index $Z(t)$ defined by projecting the daily sea-level pressure anomalies onto the NAO structure previously defined. The time series $Z(t)$ is normalized to have a standard deviation of one. Note that the NAO index has a mean of zero by construction. The NAO patterns of fields other than sea-level pressure are obtained by regressing their daily fields onto $Z(t)$. (All projections and regressions are properly area-weighted by accounting for the decrease in area toward the pole).

The NAO describes a north-south oscillation of the eddy-driven jet, with the high-phase defined as a poleward shift (anomalously low sea-level pressure over Greenland as depicted in Fig. 1) and the low-phase as an equatorward shift of the mean jet. This shift in the jet is also evident in the mass-weighted upper-level (300, 250, 200, 150 mb) relative vorticity field displayed in Fig. 2b. The high-phase NAO denotes an anomalous increase in positive vorticity to the north (compare to the winter-mean field shown in Fig. 2a), 90 degrees out of phase with the shift in upper level zonal wind. The boxed regions in Fig. 2b,c define the "north lobe" (55^o-70^oN, 310^oW-0^oE), "south lobe" (37^o-55^oN, 310^oW-0^oE), and both lobes together termed the "NAO region" (37^o-70^oN, 310^oW-0^oE) to be used in this analysis. The conclusions of this paper are robust to different regional definitions.

Fig. 2c shows the mass-weighted NAO vorticity pattern at lower levels (1000, 925, 850 mb). At these levels, the lobe over Greenland (north lobe) is significantly smaller in area than the southern lobe. The maxima of both lobes at the lower levels lie east of their respective upper-level maxima, which spread west

across the Atlantic ocean basin, indicative of a westward tilt with height.

4. Vorticity Budget

The relative vorticity tendency at a given horizontal location and vertical pressure level is given by (Holton 2004)

$$\frac{\partial \zeta}{\partial t} = -\nabla \cdot [(\zeta + f)\mathbf{u}] - \omega \frac{\partial \zeta}{\partial p} + \hat{\mathbf{k}} \cdot \left(\frac{\partial \mathbf{u}}{\partial p} \times \nabla \omega \right) + \mathcal{F}, \tag{1}$$

where $\nabla\cdot$ and ∇ denote the 2-D horizontal divergence and gradient respectively, f is the Coriolis parameter, ω is the vertical velocity, and $\mathcal{F}$ is the forcing due to friction. Using simple scaling arguments (as done in Holton (2004)), one can show that the vertical advection of vorticity and the tilting term (second and third right-hand terms) in (1) are an order of magnitude less than the convergence of vorticity flux (first right-hand term). Splitting the relevant terms in (1) into seasonal and anomalous advective and divergent quantities gives

$$\frac{\partial \hat{\zeta}}{\partial t} = -(\overline{\zeta} + \hat{\zeta} + f)\nabla \cdot (\overline{\mathbf{u}} + \hat{\mathbf{u}}) - (\hat{\mathbf{u}} + \overline{\mathbf{u}}) \cdot \nabla(\overline{\zeta} + \hat{\zeta} + f) + \mathcal{F}, \tag{2}$$

where we have made the approximation that $\frac{\partial \hat{\zeta}}{\partial t} \gg \frac{\partial \overline{\zeta}}{\partial t}$ (the climatological vorticity tendency is not identically zero due to its seasonal component). Expanding (2) and recombining to form an anomalous flux leads to

$$\frac{\partial \hat{\zeta}}{\partial t} = -(\overline{\zeta} + f)\nabla \cdot \hat{\mathbf{u}} - \nabla \cdot (\hat{\zeta}\hat{\mathbf{u}}) + \mathrm{R} + \mathcal{F}, \tag{3}$$

where R represents the neglected linear wave terms in (2). The first term on the right-hand-side of (3) is the vorticity source due to anomalous divergence, often referred to as the "stretching term". The second term represents the forcing of the anomalous vorticity due to the divergence of the anomalous vorticity flux and will be termed the "eddy forcing".

Feldstein (1998) found that high-frequency eddies extended the lifetime of a low-frequency anomaly in a GCM and that the anomaly's decay was regulated by the divergence term (similar to our stretching term). Later, he demonstrated using a reanalysis data set that the growth of the NAO was driven by the eddy fluxes and the high-frequency component prolonged its persistence, and that the divergence term was a major contributer to the NAO's subsequent decay (Feldstein 2003). With this in mind, we have chosen to

separate the stretching and the total eddy forcing from the other terms and propose that the large-scale NAO vorticity pattern organizes the anomalous eddy-vorticity flux divergence to balance surface drag in such a way as to prolong the lifetime of the NAO anomalies. Further justification for separating the terms in this way will be provided in the next two sections.

5. Feedback mechanism

We hypothesize a feedback mechanism that compensates for the effect of surface drag and enables persistence and self-maintenance of the NAO pattern. Fig. 3 depicts the proposed mechanism for a region of anomalous positive vorticity, with the anomalous westerly zonal wind located equatorward of the vorticity anomaly. The eddy vorticity flux converges at upper levels to reinforce the positive vorticity anomaly associated with the NAO. The convergence of eddy vorticity flux is balanced by divergence aloft that produces a vorticity sink through the stretching term. This divergence of mass at upper levels requires an upward velocity in this region and, thus, mass convergence at the surface which maintains the vorticity anomaly against friction via stretching. The eddy vorticity flux convergence at upper levels thus acts to sustain the vorticity anomaly associated with the NAO against surface drag, and hence increases the persistence of the NAO vorticity anomaly.

The vertical motion we associate with the convergence due to the stretching term can be likened to Ekman pumping. The adiabatic cooling due to this vertical circulation cools in the right locations to offset eddy heat fluxes and maintain thermal wind balance associated with the shift of the vorticity anomalies. This is analogous to Robinson's (2006) argument for why eddy-driven jets can be self-sustaining. If the eddies associated with the jet propagate meridionally away from the region of strongest baroclinicity before breaking, one expects a stronger equilibrium temperature gradient from the weakened heat transport by the residual circulation (Hartmann 2007). The increased baroclinicity in this region generates more eddies, which act to sustain the jet.

The three-dimensional NAO structure is not entirely barotropic but rather has a slight westward tilt with height; its shape changes with altitude also. The structure in the upper troposphere differs from that at the

surface (compare Fig. 2b,c), where surface drag damps the anomalies. Because of the need to balance the effect of surface drag, our analysis focuses on the lower-level anomaly structure.

The analysis described utilizes mass-weighted upper- and lower-level fields, averaged for levels 300, 250, 200, 150 mb and 1000, 925, 850 mb respectively. The following results are robust in that pairing any upper and lower level and performing the analysis produces similar conclusions (results not shown). Analysis at pressure levels outside of these seven levels reveals weak/insignificant feedbacks due to a lack of divergence (result of mass conservation) in the middle of the troposphere.

6. Vorticity-eddy feedback of the NAO

In a zonal-mean, vertically-averaged framework, LH01 found that the zonal index and its eddy forcing closely follow the differential equation:

$$\frac{dz}{dt} = m - \frac{z}{\tau}, \tag{4}$$

where m is the zonal-mean eddy-forcing time series, z is the index of the annular mode, and τ is a decay time scale. In this section, we investigate the feedback between the NAO and eddy forcing using the logic of LH01, but applied to the local 3-D structure of the NAO.

a. Definition of forcing time series

We project the lower-level EOF pattern onto the upper-level divergence of eddy vorticity flux to obtain the forcing time series $M(t)$, which is then normalized to have a standard deviation of one (note that M has a zero mean by construction).

By defining the forcing time series $M(t)$ in this way, we have implicitly assumed that the optimal shape of the eddy vorticity convergence for forcing the NAO anomaly is the shape of the NAO vorticity anomaly itself. It is not obvious that the best way to force a wave is to use in-phase forcing since advection is present. The following heuristic argument suggests why this may be appropriate for a steady Rossby wave.

Consider the stationary vorticity equation for a simple background zonal flow,

$$\overline{u}\frac{\partial\hat{\zeta}}{\partial x} + \beta\hat{v} = \mathcal{S} - \alpha\hat{\zeta}. \tag{5}$$

Here, drag is parameterized as a linear function of the anomalous vorticity and $\mathcal{S}$ represents a vorticity source. Defining the stream function $\psi(x)$ as $\zeta = \nabla^2\psi$ and decomposing into Fourier components using $\psi(x,y) = \tilde{\psi}(k,l)e^{(kx+ly)}$ and looking at the resonant mode where $\overline{u} = \beta(k^2+l^2)^{-1}$, one can obtain

$$\tilde{\psi} \sim \frac{-\tilde{\mathcal{S}}}{\alpha(k^2+l^2)}, \qquad \tilde{\zeta} \sim \frac{\tilde{\mathcal{S}}}{\alpha}. \tag{6}$$

Therefore, under the assumption that the wave is approximately stationary and resonant, it is plausible that in-phase forcing will efficiently reinforce the wave. Further analysis of this question is beyond the scope of the present work.

A positive feedback implies that the *lower-level* NAO vorticity anomaly be sustained by the the *upper-level* eddy forcing anomaly. We project the lower-level EOF pattern onto the upper-level vorticity, calling the resulting time series $Y(t)$. This time series captures the structure within the upper level vorticity pattern that can best balance the low-level drag. Thus, our hypothesis implies that

$$\frac{dY}{dt} = M - \frac{Y}{\tau}. \tag{7}$$

In support of this mechanism, Fig. 4a shows the NAO structure obtained by regressing Z onto the mass-weighted, upper-level stretching term. In the mid-latitudes, the upper-level stretching pattern organizes over the eastern Atlantic basin and Spain, similar to the lower-level NAO structure in Fig. 2c, although of opposite sign to balance surface drag. The lower-level divergence induces a negative vorticity tendency, which sustains the negative vorticity anomaly against drag. In the higher latitudes over Greenland, this term does not project well onto the lower-level structure, although divergence occurs east of the anomaly.

Fig. 4b depicts the total eddy-forcing projection. Although the field is significantly noisier than the upper-level divergence, it exhibits convergence of eddy vorticity flux in the polar regions and divergence in the mid-latitudes. We expect this term to be in phase with the upper-level NAO anomaly in order to cancel the anomalous divergence at this level.

It is interesting to separate the "synoptic" (high-frequency) eddy forcing from the total forcing (Fig. 4b). This is done by high-pass ($<$ 7 day) filtering the anomalous horizontal winds ($\mathbf{u}'$) and the vorticity

($\zeta^{'}$) and computing the component of the eddy forcing due to fluctuations on these synoptic time scales ($-\nabla \cdot (\zeta^{'}\mathbf{u}^{'})$). The resulting projection of the synoptic eddy forcing onto the NAO time series is shown in Fig. 4c. The vorticity tendency due to the synoptic eddy forcing aligns well with the upper-level NAO vorticity structure over the mid-latitudes and over Greenland. This result is consistent with previous studies, where the importance of synoptic eddies in driving and maintaining large-scale variability in the atmosphere has been demonstrated (Nakamura and Wallace 1990; Branstator 1992; Lorenz and Hartmann 2001; Feldstein 2003; Eichelberger and Hartmann 2007). Robinson (1991) found evidence of a feedback between synoptic waves and vorticity anomalies in a simple GCM. He concluded that the eddies both reinforced the low-frequency structures as well as slowed their eastward propagation. The projection shown in Fig. 4c supports the hypothesis that the synoptic eddies are acting to sustain the large-scale NAO structure. We quantify this argument in the next section.

b. Feedback Analysis

Fig. 5a shows the cross-correlation between M and Y for the Atlantic region, with positive lags signifying that Y leads M. As discussed in LH01, positive correlations at lags larger than a typical synoptic disturbance (7 days) imply a positive feedback between the eddy forcing and the slowly varying vorticity field. For the total eddy forcing, M is positively correlated with Y at the 95% confidence level for lags 5-11 days (see Appendix A for details). These positive correlations support the hypothesis that the NAO anomalies lead the total eddy forcing, and thus the low-frequency structures organize the eddy fluxes for self-maintenance.

One might argue that the positive correlations at positive lags are due purely to the memory of the eddies themselves and are not a reflection of the NAO anomalies organizing the eddies. To confirm that this is not the case, we repeat the correlation analysis for the high-frequency eddy forcing ($-\nabla \cdot (\zeta^{'}\mathbf{u}^{'})$) and the residual eddy forcing defined as the total field minus the high-frequency. The resulting cross-correlations are also plotted in Fig. 5a. It is clear from this curve that the synoptic eddies are the source of the positive cross-correlations between the vorticity anomalies and the total eddy forcing. Since the synoptic eddies fluctuate on time scales shorter than 7-days, and yet they account for the positive correlations at lags up to 20 days, the vorticity structure must be organizing the synoptic eddies. Hence, the net positive feedback

between the eddies and the NAO vorticity anomalies is driven by the high-frequency eddy fluxes.

It could be argued that the positive eddy-feedback is small compared to the effects of the other terms in R and the stretching term from (3). To show the importance of the eddy terms with respect to all the other terms in the vorticity tendency equation, we plot the cross-covariance of Y with the forcing time series of the total eddy term, the synoptic eddy term and all residual terms (R + stretching) in Fig. 5b. The synoptic eddy forcing contributes substantially to the total vorticity forcing at all lags, and the total eddy forcing is seen to dominate the other forcing terms at lags beyond 5 days. Thus, although the relative magnitude of the eddy forcing is smaller than the other forcing terms (not shown), only the eddy forcing is coherent with the NAO anomaly itself at large positive lags and contributes importantly to increasing the persistence of the NAO.

c. Importance of feedback in the mid-latitudes

Applying the previous analysis to the north and south lobes individually (as defined in Fig. 2b,c), we find that only the south (mid-latitude) lobe of the NAO anomalous vorticity participates in the positive feedback mechanism. Fig. 6a shows lagged correlations for the north and south lobes individually. Here, correlations for the south lobe between 0-16 days lie above the 95% confidence level while only day 9 satisfies this criteria in the north lobe. This result appears robust to the region definitions, although increasing the south lobe region much beyond the scale of the surface vorticity anomaly causes the results to fall below the calculated confidence level (due to an increase of locations not encompassed by the NAO anomaly).

Further evidence of the lack of feedback in the north lobe appears in the projections of the upper-level divergence and eddy forcing (see (3)) at the onset of the NAO. Fig. 4a,b shows that the upper-level convergence of eddy vorticity flux balances the anomalous large-scale upper-level divergence only in mid-latitudes off the coast of Europe and not in the north lobe. Thus, the circulation cell required for the upper levels to support the lower-level anomalies against surface drag is not present in the north lobe of the NAO.

The difference between the two lobes can also be seen in the cross-covariances between the vorticity anomalies and the different forcings shown in the bottom two panels of Fig. 6b,c. In the north lobe, R dominates and positively forces the vorticity anomalies while the stretching term inhibits its growth and has

little effect on the anomaly's decay. The south lobe picture is very different. As already seen, the total eddy forcing is positive at large positive lags, and the stretching term negatively forces the anomaly at large lags, consistent with our proposed mechanism. In this mid-latitude region, the residual terms R, play a minor role at positive lags, unlike in the north lobe. The proposed eddy-feedback mechanism only occurs in the south lobe, while the north lobe forcing is dominated by the residual term R, which represents the linear wave terms. The largest covariance in the north lobe residual term is $-\overline{\mathbf{u}} \cdot \nabla \hat{\zeta}$ (not shown).

These findings suggest while the mid-latitude anomaly is self-sustaining due to a positive eddy feedback, the northern anomaly behaves like a propagating upper-level Rossby wave. A simple explanation for the difference between the two lobes is that the storm track (and thus abundance of synoptic eddies) lies in the mid-latitudes. Perhaps the lack of feedback in the northern lobe is simply an artifact of the lack of synoptic storms passing through. A large eddy-feedback in the south lobe is possible since there are plenty of synoptic eddies to sustain the low-frequency structure. In this interpretation, the low-frequency structure of the NAO is sustained through a positive eddy feedback and is confined to the region of synoptic activity, namely the mid-latitudes.

d. Estimation of feedback strength in south lobe

Letting $\mathcal{Y}$ and $\mathcal{M}$ denote the Fourier transforms of Y (lower-level pattern regressed onto upper-level vorticity) and M (eddy forcing time series) respectively, we define the transfer function between Y and M to be

$$\frac{\mathcal{M}(\omega)\mathcal{Y}^*(\omega)}{\mathcal{Y}(\omega)\mathcal{Y}^*(\omega)} = \frac{1}{\tau} + i\omega, \tag{8}$$

where ω denotes the angular frequency and * signifies the complex conjugate. Fig. 7a shows the real and imaginary parts of the transfer function for the data over the south lobe. We focus on the south lobe since this is the region where a feedback appears to be occurring. The real part of the transfer function is approximately constant up to a frequency of 0.05 days^{-1}, and at higher frequencies the noise in the real part starts to dominate. The imaginary part of the transfer function follows the angular frequency (as predicted by theory (8)), up to a frequency of about 0.125 days^{-1}. Using the fact that our calculated transfer function follows the predicted behavior for low frequencies below 1/20 days^{-1}, we follow the method outlined in LH01

(see their Appendix A) and use these curves to estimate the decay time scale $\tau = 3.8$ days. This time scale represents the e-folding time of the time series Y if the eddies did not force the NAO anomaly. LH03 followed this same method and calculated a decay time scale of 6.8 days for the Northern Hemisphere Annular Mode calculated from zonal-mean data. The fact that our calculated time scale is about 1.75 times smaller than that of LH03 indicates that the zonal-mean, hemispheric mode would persist longer than the regional NAO in the absence of a feedback.

We can quantitatively estimate the strength of the eddy-feedback in the south lobe of the NAO under the assumption that the eddy forcing produced is proportional to the vorticity anomalies. We model the eddy-forcing time series M such that

$$M = \tilde{M} + bY, \tag{9}$$

where $\tilde{M}$ is a random forcing. We have an equivalent equation to (7) for $\tilde{Y}$, the time series of the lower-level pattern projected onto the upper-level vorticity absent a feedback:

$$\frac{d\tilde{Y}}{dt} = \tilde{M} - \frac{\tilde{Y}}{\tau}. \tag{10}$$

Following the method outlined by LH01 (see their Appendix C), the south lobe feedback parameter b is 0.19. Now that we have quantified the feedback between the eddy forcing and the vorticity anomaly, $\tilde{M}$ and $\tilde{Y}$ can be calculated and used to compute the cross-correlations without the feedback and the power spectrum of $\tilde{Y}$ without the feedback, as shown in Fig. 7b,c. The cross-correlation curves show that without the feedback, the correlation at positive lags drops to zero (by construction in the calculation of b). Comparing these cross-correlations with those of Y and M in the north lobe (Fig. 6b), we see that both curves have near-zero correlations by 5 days and behave similarly at both positive and negative lags. Looking at the power spectra of Y and $\tilde{Y}$ (Fig. 7c) it is clear that the power at low frequencies is greatly reduced with the removal of the feedback, indicating that the feedback between the synoptic eddies and the anomaly accounts for much of the persistence of the NAO anomalies in the mid-latitudes.

7. Asymmetry between phases of the NAO

Nakamura and Wallace (1991) documented the skewness of the 500 mb geopotential height field, indi-

cating a region of positive skewness poleward of the Atlantic storm track and a region of negative skewness equatorward. Recently, Rennert and Wallace (2009) suggested that the skewness in the 500 mb geopotential height field results from the coupling between the variability on intermediate (6-30 days) and long (30+ days) time scales. Consistent with these results, Woollings et al. (2008, 2009) highlighted the robust nature of the well-known negative skewness of the NAO time series. A negative skewness (-0.19 for our Z) implies more extreme negative values than positive and more positive values than negative overall. They presented a synoptic-regime explanation, where the low-phase NAO is interpreted as a regime with Atlantic blocking and the high-phase as a regime without. They demonstrated significantly more negative-phase NAO events (when the NAO index is below -1) lasting 10 days than would be expected by a simple AR1 model. The positive-phase NAO events (when the NAO index is above $+1$) behaved similarly to an AR1 process, supporting their synoptic view.

In this section, we present a simple measure of the persistence of the NAO phases and show that the low-phase has an extended persistence compared to that of the high-phase. Applying our eddy-feedback analysis to each phase individually, we find a stronger positive eddy feedback for the low-phase than the high-phase, consistent with the extended persistence of the low-phase.

a. Persistence of NAO phases

Compositing the upper-level vorticity field on days when Z falls into its upper 5% or lower 5% leads to a remarkable difference between the two phases. Fig. 8 displays these composites at NAO peak (lag 0 days) and 15 days later. The low phase NAO structure 15 days after a peak in Z greatly resembles that at lag 0 days, while the high phase NAO structure appears significantly weaker and less organized. Similar results emerge when we composite the zonal winds, sea-level pressure and geopotential height fields at upper-levels at large lags. This raises the question, does the low phase of the NAO have a significantly greater persistence than the high phase?

To explore the persistence of the difference phases, we follow Woollings et al. (2009) and define a run statistic for the different phases of the NAO. The duration of a high-phase (low-phase) NAO event is defined by the number of consecutive days Z is above (below) $+1$ (-1). Instead of plotting the number of runs as

done by Woollings et al. (2009), we analyze the frequency of events with durations equal to or exceeding n days, defined as the number of runs normalized by the total number of distinct events in the associated phase (223 [137] events for the high [low] phase). We choose to analyze frequency instead of total counts since we are not interested in whether the number of events is different between phases but rather if low-phase events last longer. Fig. 9 displays the results, where the gray shading denotes the 95% confidence limit that the frequency of events lasting at least n days is significantly higher during the low-phase NAO (see Appendix B for calculations). We find that significantly more events have minimum durations of 2-27 days for the low-phase than the high-phase, consistent with Fig. 8. These results do not contradict Woollings et al. (2009) who found that the low-phase NAO durations did not behave like an AR1 process for events lasting 10 days while the high-phase did. Rather, our results state that even if the two phases of the NAO behave as AR1 processes, they are *different* AR1 processes.

It is important to note that the skewness of Z alone is not an appropriate measure of an asymmetry in persistence. While a negative skewness is consistent with the low-phase NAO having more extreme, longer-lasting events, it is neither a necessary nor sufficient condition. One can imagine a time series of a Gaussian random variable (zero skewness) ordered such that the large-magnitude negative values are grouped together in time while the large positive values are not. Likewise, a negatively skewed time series could be ordered such that all large negative values are well separated amongst positive values, implying a lack of persistence. It is for this reason that we have investigated the difference in duration using a duration statistic.

b. Feedbacks of the high- and low-phase NAO

We have established that low-phase NAO events persist for longer periods of time than high-phase. Could this asymmetry in persistence be due to a difference in eddy feedback strength? To address this question,

we separate Z into a high (Z_+) and low (Z_-) index in the following way:

$$Z(t)_+ = \begin{cases} Z(t) & \text{if } Z(t) > 0, \\ 0 & \text{otherwise.} \end{cases}$$

$$Z(t)_- = \begin{cases} Z(t) & \text{if } Z(t) < 0, \\ 0 & \text{otherwise,} \end{cases} \tag{11}$$

For notational clarity, we will define the variables t_+ and t_- as the days when Z_+ and Z_- are non-zero, respectively. This leads to t_+ containing 2736 days and t_- containing 2478 days.

We wish to apply the same method as in previous sections to investigate a positive feedback between the eddy forcing and the two phases of the NAO. We define the lower-level high- (low-) phase NAO pattern as the projection of the lower-level daily relative vorticity onto Z_+ (Z_-). As one might expect, the two patterns are nearly identical but of opposite sign (not shown). As before, we wish to compare the upper-level vorticity field with the lower-level NAO response; thus, $Y_+(t)$ ($Y_-(t)$) is defined as the projection of the high- (low-) phase NAO pattern onto the upper-level relative vorticity on days t_+ (t_-).

Lastly, we must define the eddy forcing time series for the different phases. Since one expects the response of the eddy forcing to lag the large-scale circulation (as seen in the full NAO feedback case), we cannot simply define the eddy forcing time series on days t_+ and t_-. Rather, $M_+(t)$ ($M_-(t)$) is defined as the projection of the lower-level high- (low-) phase pattern onto the upper-level eddy forcing field for *all* days. Although the high- and low-phase relative vorticity structures are not identical, the forcing time series $M_+(t)$ and $M_-(t)$ are correlated at 0.96. This high correlation is expected since the NAO structures at lower levels for the high- and low-phases are nearly identical in shape.

Fig. 10 shows the cross-correlations between M_+ and Y_+ and between M_- and Y_- in the south lobe. At positive lags, the low-phase correlation is statistically different from zero for lags 0-14 days at 95% confidence. The high-phase correlation is only significant at lags of 3-7 days. The high-phase NAO lacks the positive eddy feedback beyond a single eddy lifetime. To confirm that the synoptic eddies contribute to this asymmetry, Fig. 10b shows the cross-covariance for the synoptic eddies only as well as the stretching term. The low-phase NAO has positive covariances at positive lags beyond 7 days while the high-phase does not.

We have verified that the non-synoptic eddies contribute similar magnitudes for both phases, implying that the asymmetry in the total eddy forcing is due purely to the synoptic eddy component. Consistent with our proposed feedback mechanism, the stretching term negatively forces the vorticity anomalies at upper-levels for both phases. Plots of correlation (not shown) show similar results, implying that the differences in Fig. 10b are not merely due to a difference in variance between the two phases.

To investigate the reason for the apparent asymmetry in feedback between the two NAO phases, we compute the vector $\mathbf{E} = (v^{'2} - u^{'2}, -u^{'}v^{'})$ which corresponds to the horizontal components of the high-frequency **E**-vector defined by Hoskins et al. (1983). The vector may be interpreted as an effective momentum flux, and its horizontal divergence gives the forcing of the background flow by the synoptic eddies. We composite the horizontal **E**-vectors and the vertically-averaged zonal wind for the top and bottom 5% of the NAO index Z and plot the result in Fig. 11. The high-phase composite wind shows a clear poleward shift of the jet while an equatorward shift of the jet is evident in the low-phase. A remarkable difference between the two phases is the location and direction of the eddy propagation away from the jet. In the low-phase, the eddies turn preferentially poleward over the mid-Atlantic. In the high-phase, the eddies propagate along the axis of the jet and then break equatorward over Eastern Europe. The high-phase has a larger magnitude eddy-forcing over Europe due to the stronger winds. However, the main region of action for the NAO is over the Atlantic Ocean, where during the low-phase, eddies transport wave-activity poleward away from the jet and transport momentum back into the jet.

Fig. 11 implies that the weak zonal flow of the low-phase NAO blocks the eastward propagation of the synoptic eddies, unlike in the high-phase where the eddies break in a broad region downstream of the Atlantic. To quantitatively support this explanation, we define a replacement time scale τ_R, which represents the amount of time it would take a given vorticity tendency (forcing terms on the r.h.s of (3)) to replace the existing vorticity anomaly (ζ_{nao}). Mathematically, this is:

$$\tau_R = \frac{\overline{\zeta_{nao}^2}}{\zeta_{nao}\overline{\frac{\partial\hat{\zeta}}{\partial t}}_{HF}}, \tag{12}$$

where $\partial\hat{\zeta}/\partial t_{HF}$ is the vorticity tendency associated with the high-frequency (synoptic) eddies. We define τ_R for the low- and high-phases by compositing the upper-level vorticity anomaly and vorticity tendency due to the synoptic eddies over the top and bottom 5% of the NAO time series Z. τ_R is then defined as the

ratio of the area-average square vorticity anomaly to the area-average product of the vorticity anomaly and the vorticity tendency. In the south lobe region, the resulting time scales are 7.7 days and 3.5 days for the high- and low-phases respectively. The shorter time scale for the low-phase implies that the synoptic eddies replace the low-phase vorticity anomaly at a faster rate than do those during the high-phase. Calculations of τ_R in the Atlantic sector and the NAO region also show shorter replacement time scales for the low-phase than for the high-phase, although the greatest difference between the two-phases is found in the south lobe, consistent with a stronger eddy feedback in the mid-latitudes.

Both the **E**-vectors and the replacement time scales demonstrate the greater synoptic eddy feedback found during the low-phase NAO. We argue that although the magnitude of the eddies during the low-phase is small in comparison to those of the high-phase, their propagation due to the weak flow associated with the low-phase NAO better aligns and reinforces the NAO anomaly. This mechanism is also consistent with the work of Woollings et al. (2008, 2009) who argue that blocking events in the Atlantic characterize the low-phase NAO, whereas the high-phase is purely a lack of blocking anticyclones. Using the methodology described here, we can show how the altered transient eddy fluxes contribute persistence to the low phase of the NAO.

8. Summary

Analysis of the vorticity tendency equation in the upper-troposphere and near the surface has demonstrated that a positive feedback exists between the eddies and the vorticity anomalies associated with the NAO. The convergence of synoptic eddy-vorticity flux at upper levels counteracts the effects of the large-scale divergence. At the lower levels, the large-scale convergence associated with the induced vertical circulation cell positively forces the lower-level NAO anomaly and thus sustains the anomaly against frictional drag. Our proposed feedback mechanism is consistent with that of a self-sustaining jet as discussed by Robinson (2006), where the cooling and warming due to vertical motion offset the eddy heat flux anomalies.

While the upper-level divergence and total eddy forcing are dominant in the total vorticity budget in the mid-latitude lobe of the NAO, the residual terms dominate in the northern anomaly over Greenland. This

implies that the persistence of the NAO in the mid-latitudes can be explained by a positive eddy-feedback while the northern lobe has no feedback with the eddies and acts as a propagating Rossby wave. The lack of feedback in the lobe over Greenland and presence of feedback in the mid-latitude lobe can be understood by the positioning of the eddy paths, or storm tracks. Where there is an abundance of eddies (passing storms), a positive feedback between the eddies and the low-frequency pattern of the NAO is observed. However, over Greenland, there is no feedback as this region is outside of the domain of the climatological storm track.

The NAO is often viewed as a linear oscillation/shift of the jet-stream to its north and south, but we have shown that low-phase NAO events last significantly longer than high-phase NAO events. In other words, once the jet has shifted equatorward, it stays in this configuration for longer periods of time than when it is poleward of its climatological position. Applying our eddy-feedback framework to this asymmetry, we showed that the low-phase NAO exhibits a larger eddy feedback than the high-phase, consistent with the its extended persistence. Composites of vertically-averaged, high-frequency **E**-vectors for the the two phases show the difference in eddy propagation in the mid-latitudes. The eastward propagation of the eddies in the low-phase NAO tends to be blocked in the mid-Atlantic, causing them to turn and propagate preferentially poleward, fluxing momentum into the jet. However, in the high-phase, the eddies propagate eastward over the Atlantic and do not turn equatorward until they are over Europe, far downstream of the NAO anomaly, and the eddy flux convergence is less concentrated. To demonstrate this quantitatively, we calculated the replacement time of the mid-latitude NAO vorticity anomaly by the vorticity tendency due to the synoptic eddy forcing. The low-phase time was half as long as that of the high-phase, implying that the synoptic eddies replace the low-phase NAO vorticity anomaly at a much faster rate, consistent with a stronger eddy feedback. In this framework, the eddies in the high-phase do not reinforce the NAO anomaly as much due to their extended downstream propagation, while the weak zonal flow associated with the low-phase NAO induces the eddies to break in the region of the anomaly, reinforcing the NAO pattern.

Acknowledgments.

We would like to thank John M. Wallace and Dargan Frierson for their helpful suggestions and Randal J. Barnes for his aid in developing the statistical framework. This work supported by the Climate Dynamics

Program of the National Science Foundation under grant ATM 0409075.

APPENDIX A

Cross-correlation statistics

We define $\hat{\rho}(h)$ as the estimated cross-correlation between the two time series Y and M each composed of $W = 43$ winter seasons of $d = 121$ days each. To simplify the formulas, we let $Y = Y(d, w)$ which denotes the dth day of the wth winter-season. Then, $\hat{\rho}$ is estimated by

$$\hat{\rho}(h) = \frac{\sum_{w=1}^{43} \sum_{d=1}^{121-h} (Y(d,w) - \mu_Y) \cdot (M(d+h,w) - \mu_M)}{43(121-h) \cdot \sqrt{\nu_Y(h)\nu_M(h)}}, \tag{A1}$$

where μ_Y and μ_M are the arithmetic averages of Y and M over all winter days, and $\nu_Y(h)$ and $\nu_M(h)$ are the estimated variances at lag h defined by

$$\nu_Y(h) = \frac{1}{43(121-h)} \sum_{w=1}^{43} \sum_{d=1}^{121-h} (Y(d,w) - \mu_Y)^2 \tag{A2}$$

$$\nu_M(h) = \frac{1}{43(121-h)} \sum_{w=1}^{43} \sum_{d=1}^{121-h} (M(d+h,w) - \mu_M)^2. \tag{A3}$$

Note that if the cross-correlations were normalized by $(43 \cdot 121)^{-1}$, $\mu_Y = \mu_M = 1$ by construction.

The method to asses the statistical significance of the cross-correlations directly follows that outlined by Lorenz and Hartmann (2001). We perform a Monte Carlo simulation to test the following null hypothesis: the cross-correlation is zero at positive lags. We generate 1000 random forcing time series $\hat{M}$ (5214 days each split into 121 day seasons) using a moving average model with parameters θ_i. These parameters are estimated from the autocorrelation of the real forcing time series M up to lag 6 (where the autocorrelation drops to near zero) using the iterative method outlined by Box et al. (2008). We calculate the corresponding $\hat{Y}$ (model time series of Y) using (7) with the complimentary $\tau = 3.8$ days (see Appendix A of Lorenz and Hartmann (2001)). Calculating the cross-correlations for each of the 1000 sets of $\hat{M}$ and $\hat{Y}$ and computing the 95th percentile correlation at positive lags gives a 95% significance value of 0.023.

APPENDIX B

Statistical significance of duration

We model the NAO time series Z as a strictly stationary, zero-mean, AR1 process with parameters ϕ and σ (Box et al. 2008). The model time series $\hat{X}$ has 43 chunks of 121 days each (similar to Z). Although the NAO time series Z has zero mean, each winter-mean NAO index is *not* zero. Thus, we adjust our model time series to incorporate non-zero seasonal-mean values and denote this final model time series as X. Letting d denote the day within a winter season, w the specific winter season, and $\mathcal{W}(w)$ the mean-seasonal value estimated from the wth season of Z, we obtain

$$\hat{X}(d,w) = \quad \phi \cdot \hat{X}(d-1,w) + \epsilon(d) \tag{B1}$$

$$\begin{aligned} X(d,w) &= \quad \hat{X}(d,w) + \mathcal{W}(w) \\ &= \quad \phi \cdot \tilde{X}(d-1,w) + \epsilon(d) + \mathcal{W}(w), \end{aligned} \tag{B2}$$

where ϵ is white noise with variance σ. To estimate the parameters σ and ϕ from the data, a modified NAO time series is defined:

$$\hat{Z}(d,w) = Z(d,w) - \mathcal{W}(w). \tag{B3}$$

Using $\hat{Z}$, we estimate the AR1 parameters:

$$\phi = \frac{\sum_{w=1}^{43}\sum_{d=2}^{120} \hat{Z}(d-1,w)\cdot\hat{Z}(d,w)}{\sum_{w}\sum_{d}\hat{Z}(d,w)^2} \tag{B4}$$

$$\sigma^2 = \frac{1}{(43\cdot 120)}\sum_{w=1}^{43}\sum_{d=2}^{121}\Big(\hat{Z}(d-1,w) - \phi\cdot\hat{Z}(d,w)\Big)^2. \tag{B5}$$

We wish to calculate a 95% confidence interval for the difference between the frequency of minimum duration for the high- and low-phases of the NAO under the null hypothesis that the low- and high-phase runs have the same duration distributions. We create 10000 model time series X as described above. The duration of a high-phase (low-phase) NAO event is defined as the number of consecutive days Z is above

(below) +1 (-1). For each time series, we compute the frequency of events with durations equal to or exceeding n days for both low- and high-phase events (as explained in the text). The 95%tile of the difference between the low and high phase curves gives the 95% confidence interval for the difference. These calculations show that a higher frequency of occurrence of long-lasting low-phase events exist than for the high-phase events for durations 2-27 days.

REFERENCES

Ambaum, M., B. Hoskins, and D. Stephenson, 2001: Arctic Oscillation or North Atlantic Oscillation? *J. Climate*, **14**, 3495–3507.

Box, G. E. P., G. M. Jenkins, and G. C. Reinsel, 2008: *Time Series Analysis: Forecasting and Control*. 4th ed., John Wiley & Sons, Inc., 746 pp.

Branstator, G., 1992: The maintenance of low-frequency atmospheric anomalies. *J. Atmos. Sci.*, **49**, 1924–1945.

Eichelberger, S. J. and D. L. Hartmann, 2007: Zonal jet structure and the leading mode of variability. *J. Climate*, **20**, 5149–5163, doi:10.1175/JCLI4279.1.

Feldstein, S. B., 1998: The growth and decay of low-frequency anomalies in a GCM. *J. Atmos. Sci.*, **55**, 415–428.

Feldstein, S. B., 2000: The timescale, power spectra, and climate noise properties of teleconnection patterns. *J. Climate*, **13**, 4430–4440.

Feldstein, S. B., 2003: The dynamics of NAO teleconnection pattern growth and decay. *Quart. J. Roy. Meteor. Soc.*, **129**, 901–924.

Feldstein, S. B. and S. Lee, 1998: Is the atmospheric zonal index driven by an eddy feedback? *J. Atmos. Sci.*, **55**, 3077–3086.

Hamming, R. W., 1989: *Digital Filters*. Prentice Hall, 284 pp.

Hartmann, D. L., 2007: The atmospheric general circulation and its variability. *J. Meteor. Soc. Japan*, **85B**, 213–143.

Holopainen, E. O. and A. H. Oort, 1981: On the role of large-scale transient eddies in the maintenance of the vorticity and enstrophy of the time-mean atmospheric flow. *J. Atmos. Sci.*, **38**, 270–280.

Holton, J. R., 2004: *An Introduction to Dynamic Meteorology*. 4th ed., Elsevier Academic Press, 535 pp.

Hoskins, B. J., I. N. James, and G. H. White, 1983: The shape, propagation and mean-flow interaction of large-scale weather systems. *J. Atmos. Sci.*, **40**, 1595–.

Lorenz, D. J. and D. L. Hartmann, 2001: Eddy-zonal flow feedback in the Southern Hemisphere. *J. Atmos. Sci.*, **58**, 3312–3327.

Lorenz, D. J. and D. L. Hartmann, 2003: Eddy-zonal flow feedback in the Northern Hemisphere winter. *J. Climate*, **16**, 1212–1227.

Nakamura, H. and J. M. Wallace, 1990: Observed changes in baroclinic wave activity during the life cycles of low-frequency circulation anomalies. *J. Atmos. Sci.*, **46**, 1100–1116.

Nakamura, H. and J. M. Wallace, 1991: Skewness of low-frequency fluctuations in the tropospheric circulation during the Northern Hemisphere winter. *J. Atmos. Sci.*, **48**, 1441–1118.

North, G. R., T. L. Bell, and R. F. Cahalan, 1982: Sampling errors in the estimation of Empirical Orthogonal Functions. *Mon. Wea. Rev.*, **110**, 699–706.

Rennert, K. J. and J. M. Wallace, 2009: Cross-frequency coupling, skewness, and blocking in the Northern Hemisphere winter circulation. *submitted*.

Robinson, W. A., 1991: The dynamics of low-frequency variability in a simple model of the global atmosphere. *J. Atmos. Sci.*, **48**, 429–441.

Robinson, W. A., 1996: Does eddy feedback sustain variability in the zonal index? *J. Atmos. Sci.*, **53**, 3556–3569.

Robinson, W. A., 2000: A baroclinic mechanism for the eddy feedback on the zonal index. *J. Atmos. Sci.*, **57**, 415–422.

Robinson, W. A., 2006: On the self-maintenance of midlatitude jets. *J. Atmos. Sci.*, **63**, 2109–2122.

Thompson, D. W. and J. M. Wallace, 1998: The Artic Oscillation signature in the wintertime geopotential height and temperature fields. *Geophys. Res. Lett.*, **25**, 1297–1300.

Thompson, D. W. and J. M. Wallace, 2000: Annular modes in the extratropical circulation. Part I: Month-to-month variability. *J. Climate*, **13**, 1000–1016.

Uppala, S. M., et al., 2005: The ERA-40 reanalysis. *Quart. J. Roy. Meteor. Soc.*, **131**, 2961–3012.

Walker, G. T., 1924: Correlation in seasonal variation of weather, IX. A further study of world weather. *Mem. Ind. Met. Dept.*, **24**, 275–333.

Woollings, T., A. Hannachi, B. Hoskins, and A. G. Turnder, 2009: A regime view of the North Atlantic Oscillation and its response to anthropogenic forcing. *submitted*.

Woollings, T., B. Hoskins, M. Blackburn, and P. Berrisford, 2008: A new Rossby wave-breaking interpretation of the North Atlantic Oscillation. *J. Atmos. Sci.*, **65**, 609–626.

List of Figures

1 Leading EOF of DJFM monthly-mean sea-level pressure over the Atlantic region 90^{o}W-30^{o}E, 25-90^{o}N. Contours are drawn every 2.6 mb with negative contours dashed. The zero contour line has been omitted. 28

2 (a) Mean climatological relative vorticity at 250mb and NAO structures of relative vorticity for the mass-weighted (b) upper-level (300, 250, 200, 150 mb) and (c) lower-level (1000, 925, 850 mb) relative vorticity. Contours are drawn every 7(3.5)$\times 10^{-6}$ sec^{-1} for (a) ((b),(c)) panel with negative contours dashed. The NAO region used for the feedback analysis is overlaid with the north and south lobe regions as the north and south sectors respectively. The zero contour line has been omitted. 29

3 A schematic of the three-dimensional eddy feedback mechanism for a positive vorticity anomaly. Gray arrows represent the large-scale circulation cell set-up to balance the upper-level convergence of eddy vorticity flux and counter the dissipation of the low-level vorticity anomaly by surface drag (drag coefficient C_d). The adiabatic cooling/warming associated with the vertical motion balances the low-level temperature advection, maintaining the temperature gradient. This mechanism represents a positive feedback since the vorticity anomalies organize the upper-level eddies which act to sustain the anomalies. 30

4 NAO structures of the (a) large-scale upper-level stretching term $-(\overline{\zeta}+f)\nabla\cdot\hat{\mathbf{u}}$, (b) total eddy forcing field ($-\nabla\cdot\hat{\zeta}\hat{\mathbf{u}}$) and (c) synoptic eddy forcing only $-\nabla\cdot(\zeta^{'}\mathbf{u}^{'})$ obtained by regressing $Z(t)$ onto the field. Contours are drawn every 3$\times 10^{-11}$ sec^{-2} with negative contours dashed. The zero contour line has been omitted. 31

5 (a) Cross-correlations between Y and M in the Atlantic region for the total eddy forcing and synoptic eddy forcing. (b) Cross-covariance between Y and forcing time series for the stretching term (solid), total eddy forcing (circles) and the residual forcing (dashed) in units of sec^{-3}. In both panels, positive lags imply that Y (vorticity) leads the eddy forcing. 32

6 (a) Cross-correlation between Y and M for the south lobe and north lobe separately. (b, c) Cross-covariance between Y and forcing time series for the stretching term (solid), total eddy forcing (circles) and residual forcing R (dashed) for the north and south lobes in units of $\sec^{-3}$. In all panels, positive lags imply that Y (vorticity) leads the eddy forcing. 33

7 (a) The real and imaginary parts of the transfer function of Y and M for the south lobe. The angular frequency curve (dashed) denotes the imaginary part predicted by linear theory. (b) The cross-correlation between Y and M in the south lobe as observed and with the estimated feedback removed. (c) The power-spectrum of Y observed and with the feedback removed ($\tilde{Y}$). 34

8 (a,b) Lag 0 projections of upper-level relative vorticity for the (top, bottom) 5% of the NAO index Z. (c,d) Lag 15 days after the extreme NAO days projections of the same fields. Contours in the top (bottom) panel are drawn every $7(3.5)\times10^{-6}$ $\sec^{-1}$ with negative contours dashed. The zero contour line has been omitted. 35

9 The frequency of NAO events that last *at least* a certain number of days. A high- (low-) phase event is defined for values above (below) +1 (-1). The shading denotes the 95% confidence range that the low-index phase is significantly more persistent than the high-phase (see Appendix B for details). 36

10 (a) Cross-correlation in the south lobe between the total eddy forcing time series (M_+, M_-) and the vorticity anomaly time series (Y_+, Y_-) for the high and low indices of the NAO respectively. (b) Cross-covariance in the south lobe between the high- and low-index NAO time series and the forcing due to the synoptic eddies as well as the forcing due to the stretching term in units of $\sec^{-3}$. Positive lags imply that Y (vorticity) leads the forcing. 37

11 Composites of vertically-averaged horizontal **E**-vectors (arrows) and the vertically-averaged zonal wind (contours) for the (a) top 5% and (b) bottom 5% of the NAO index Z. Contours are drawn every 5 m·$\sec^{-1}$ with negative contours dashed. The reference vectors have magnitudes of 20 $\mathrm{m}^2\cdot\sec^{-2}$. The zero contour line has been omitted. 38

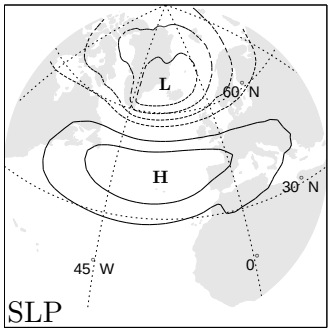

FIG. 1. Leading EOF of DJFM monthly-mean sea-level pressure over the Atlantic region 90^{o}W-30^{o}E, 25-90^{o}N. Contours are drawn every 2.6 mb with negative contours dashed. The zero contour line has been omitted.

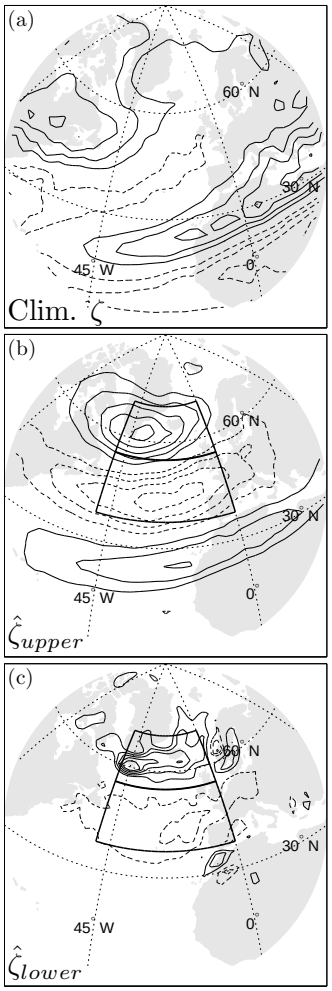

FIG. 2. (a) Mean climatological relative vorticity at 250mb and NAO structures of relative vorticity for the mass-weighted (b) upper-level (300, 250, 200, 150 mb) and (c) lower-level (1000, 925, 850 mb) relative vorticity. Contours are drawn every $7(3.5)\times10^{-6}$ sec^{-1} for (a) ((b),(c)) panel with negative contours dashed. The NAO region used for the feedback analysis is overlaid with the north and south lobe regions as the north and south sectors respectively. The zero contour line has been omitted.

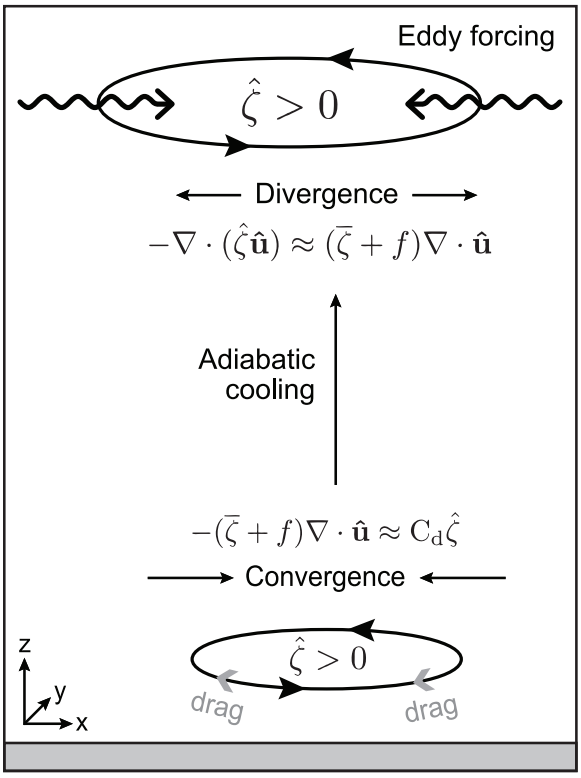

FIG. 3. A schematic of the three-dimensional eddy feedback mechanism for a positive vorticity anomaly. Gray arrows represent the large-scale circulation cell set-up to balance the upper-level convergence of eddy vorticity flux and counter the dissipation of the low-level vorticity anomaly by surface drag (drag coefficient $\mathrm{C_d}$). The adiabatic cooling/warming associated with the vertical motion balances the low-level temperature advection, maintaining the temperature gradient. This mechanism represents a positive feedback since the vorticity anomalies organize the upper-level eddies which act to sustain the anomalies.

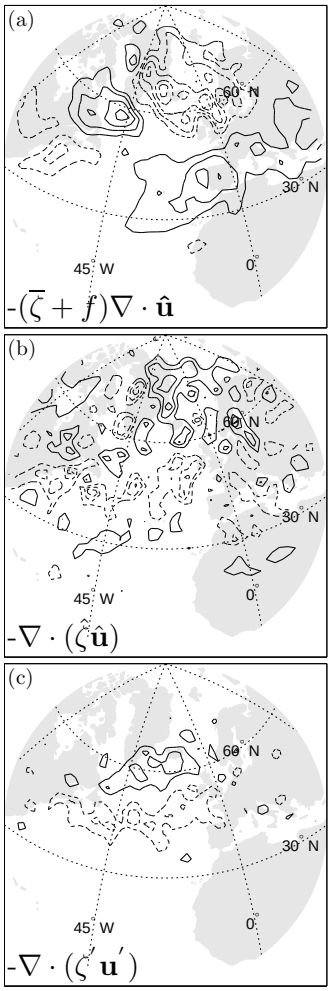

FIG. 4. NAO structures of the (a) large-scale upper-level stretching term $-(\overline{\zeta}+f)\nabla\cdot\hat{\mathbf{u}}$, (b) total eddy forcing field ($-\nabla\cdot\hat{\zeta}\hat{\mathbf{u}}$) and (c) synoptic eddy forcing only $-\nabla\cdot(\zeta^{'}\mathbf{u}^{'})$ obtained by regressing $Z(t)$ onto the field. Contours are drawn every 3×10^{-11} sec^{-2} with negative contours dashed. The zero contour line has been omitted.

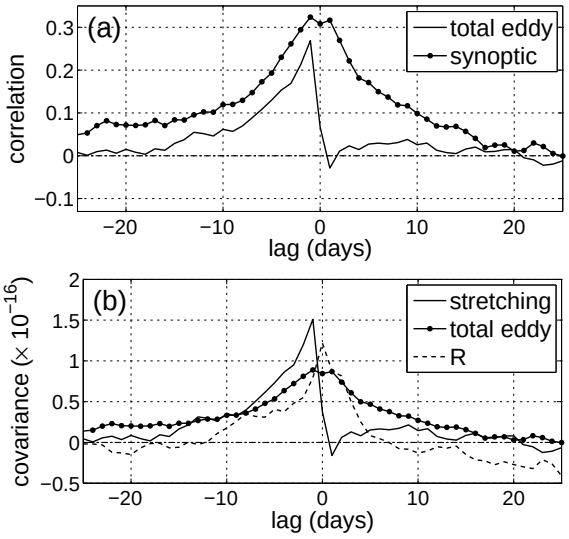

FIG. 5. (a) Cross-correlations between Y and M in the Atlantic region for the total eddy forcing and synoptic eddy forcing. (b) Cross-covariance between Y and forcing time series for the stretching term (solid), total eddy forcing (circles) and the residual forcing (dashed) in units of $\sec^{-3}$. In both panels, positive lags imply that Y (vorticity) leads the eddy forcing.

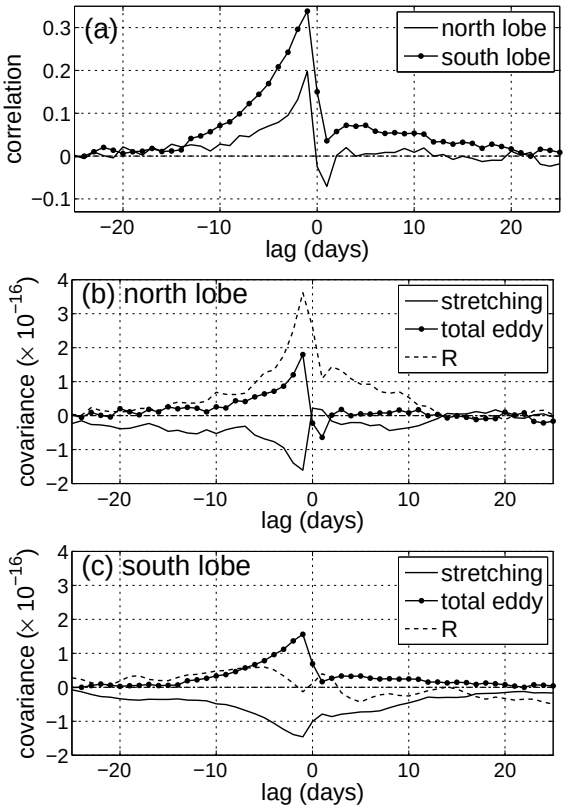

FIG. 6. (a) Cross-correlation between Y and M for the south lobe and north lobe separately. (b, c) Cross-covariance between Y and forcing time series for the stretching term (solid), total eddy forcing (circles) and residual forcing R (dashed) for the north and south lobes in units of $\sec^{-3}$. In all panels, positive lags imply that Y (vorticity) leads the eddy forcing.

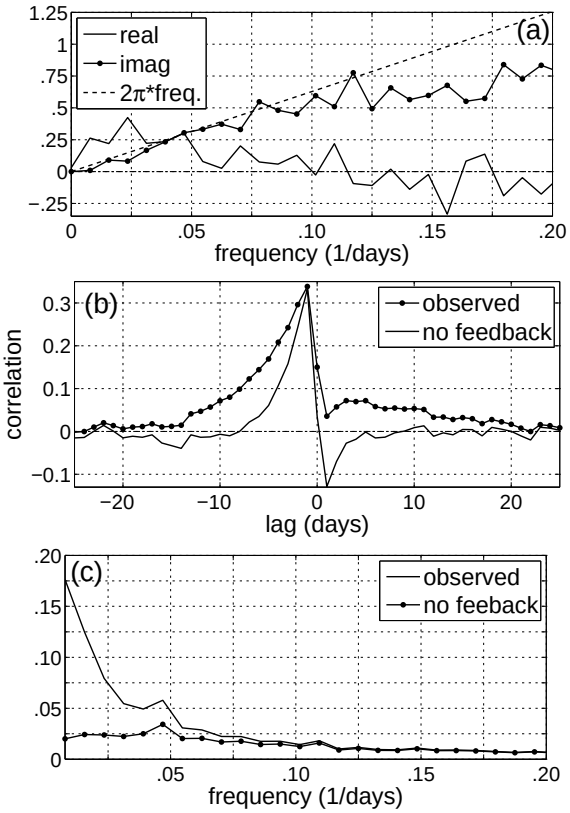

FIG. 7. (a) The real and imaginary parts of the transfer function of Y and M for the south lobe. The angular frequency curve (dashed) denotes the imaginary part predicted by linear theory. (b) The cross-correlation between Y and M in the south lobe as observed and with the estimated feedback removed. (c) The power-spectrum of Y observed and with the feedback removed ($\tilde{Y}$).

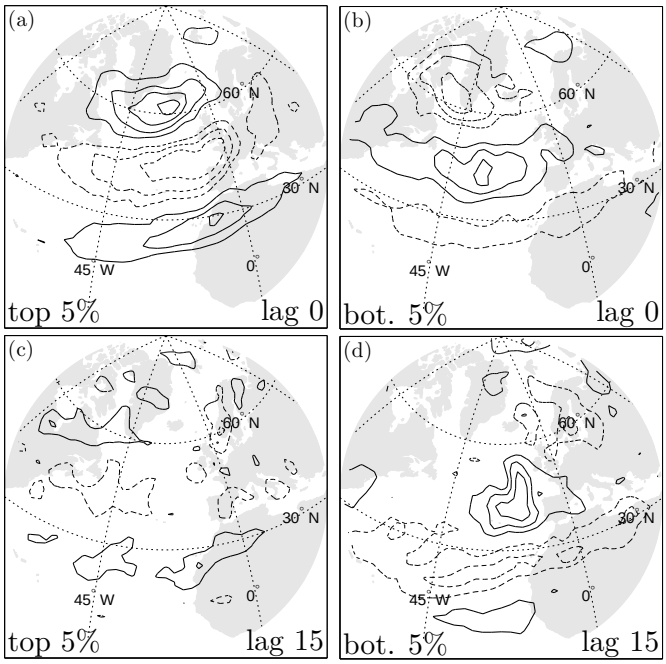

FIG. 8. (a,b) Lag 0 projections of upper-level relative vorticity for the (top, bottom) 5% of the NAO index Z. (c,d) Lag 15 days after the extreme NAO days projections of the same fields. Contours in the top (bottom) panel are drawn every $7(3.5)\times10^{-6}$ sec^{-1} with negative contours dashed. The zero contour line has been omitted.

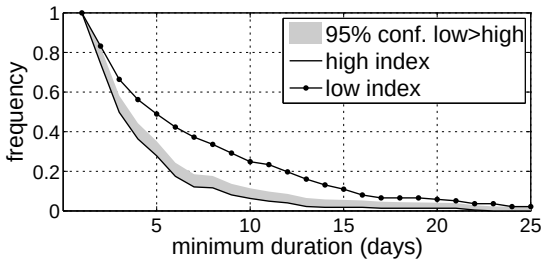

FIG. 9. The frequency of NAO events that last *at least* a certain number of days. A high- (low-) phase event is defined for values above (below) +1 (-1). The shading denotes the 95% confidence range that the low-index phase is significantly more persistent than the high-phase (see Appendix B for details).

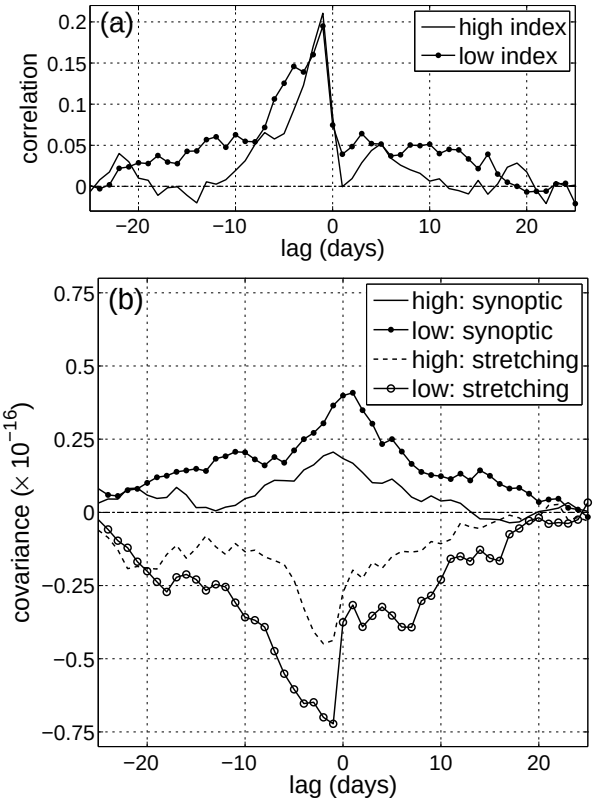

FIG. 10. (a) Cross-correlation in the south lobe between the total eddy forcing time series (M_+, M_-) and the vorticity anomaly time series (Y_+, Y_-) for the high and low indices of the NAO respectively. (b) Cross-covariance in the south lobe between the high- and low-index NAO time series and the forcing due to the synoptic eddies as well as the forcing due to the stretching term in units of $\sec^{-3}$. Positive lags imply that Y (vorticity) leads the forcing.

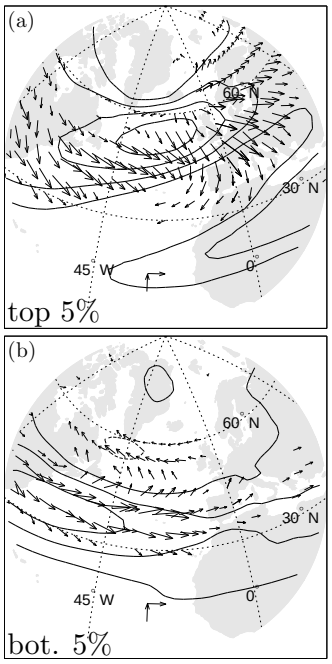

FIG. 11. Composites of vertically-averaged horizontal **E**-vectors (arrows) and the vertically-averaged zonal wind (contours) for the (a) top 5% and (b) bottom 5% of the NAO index Z. Contours are drawn every 5 m·sec^{-1} with negative contours dashed. The reference vectors have magnitudes of 20 m^2·sec^{-2}. The zero contour line has been omitted.